

# ANAPHASE PROMOTING COMPLEX/ CYCLOSOME-mediated cyclin B1 degradation is critical for cell cycle synchronization in syncytial endosperms<sup>FA</sup>

**Summary** Although it is known that in most angiosperms mitosis in early endosperm development is syncytial and synchronized, it is unclear how the synchronization is regulated. We showed previously that APC11, also named ZYG1, in *Arabidopsis* activates zygote division by interaction and degradation of cyclin B1. Here, we report that the mutation in APC11/ZYG1 led to unsynchronized mitosis and over-accumulation of cyclin B1-GUS in the endosperm. Mutations in two other APC subunits showed similar defects. Transgenic expression of stable cyclin B1 in the endosperm also caused unsynchronized mitosis. Further, downregulation of APC11 generated multi-nucleate somatic cells with unsynchronized mitotic division. Together, our results suggest that APC/C-mediated cyclin B1 degradation is critical for cell cycle synchronization.

The endosperm of seeds is the most important source of food for humans. Endosperms in most flowering plants are triploid, and arise from the fusion and divisions of one sperm and two central nuclei (Dumas and Rogowsky 2008). As a terminal tissue, the endosperm nourishes the embryo during embryogenesis and/or seed germination (Dumas and Rogowsky 2008). The early stage of endosperm development is syncytial, with mitosis of multiple nuclei in the coenocytic endosperm being highly synchronized (Dumas and Rogowsky 2008), which is similar to early embryo development in many animal species, such as *Drosophila* (Ferree et al. 2016). Although genes regulating mitotic divisions in endosperms have been reported (Liu and Meinke 1998; Liu et al. 2002; Hara et al. 2015), mutations in none of these genes have resulted in cell cycle synchronization defects. Therefore, the molecular machinery responsible for cell cycle synchronization remains largely unknown. In this study, we show that

the ANAPHASE PROMOTING COMPLEX/CYCLOSOME (APC/C) is critical for cell cycle synchronization in the endosperm of *Arabidopsis thaliana*.

Mutation of ZYGOTE-ARREST 1 (ZYG1), encoding the APC/C subunit 11 (APC11), results in a zygote-lethal phenotype (Guo et al. 2016). Here, using differential interference contrast (DIC) microscopy we examined *zyg1* endosperms from heterozygous ZYG1/*zyg1* plants, and observed that nuclei in *zyg1* endosperms were able to undergo several cycles of mitotic divisions, producing multiple coenocytic nuclei (Figures 1A, S1A). Histological analysis of 4',6-diamidino-2-phenylindole (DAPI)-stained *zyg1* endosperm sections, at 2 d after pollination (DAP), showed that mitotic divisions among these coenocytic nuclei were unsynchronized (Figure 1B), whereas mitosis in wildtype endosperms at the same developmental stage were highly synchronized (Figures 1B, S1B, S1C). The frequency of endosperms with at least one mitotic figure were 18.7% in *zyg1* ovules ( $n = 176$ ), compared to 2.3% in the wildtype ( $n = 412$ ) ( $P < 0.01$ ; Figure 1C). A gradual increase in the frequency of unsynchronized mitosis was observed in *zyg1* during the endosperm development (Figure S1B, C). These results suggest a critical role of APC11 in cell cycle synchronization in the endosperm.

To further characterize the defect in *zyg1* endosperm, we examined ovules from a heterozygous ZYG1/*zyg1* plant carrying a homozygous cyclin B1-GUS fusion construct (CYCB1-GUS; Colón-Carmona et al. 1999). Increased number and intensity of ovules with CYCB1-GUS accumulation, an indication of cell cycle arrest, were observed in *zyg1* endosperms (84.9%;  $n = 106$ ), compared to the faint GUS staining observed in wildtype-looking ovules in the same silique (1.1%;  $n = 268$ ) ( $P < 0.01$ ; Figure 1D).

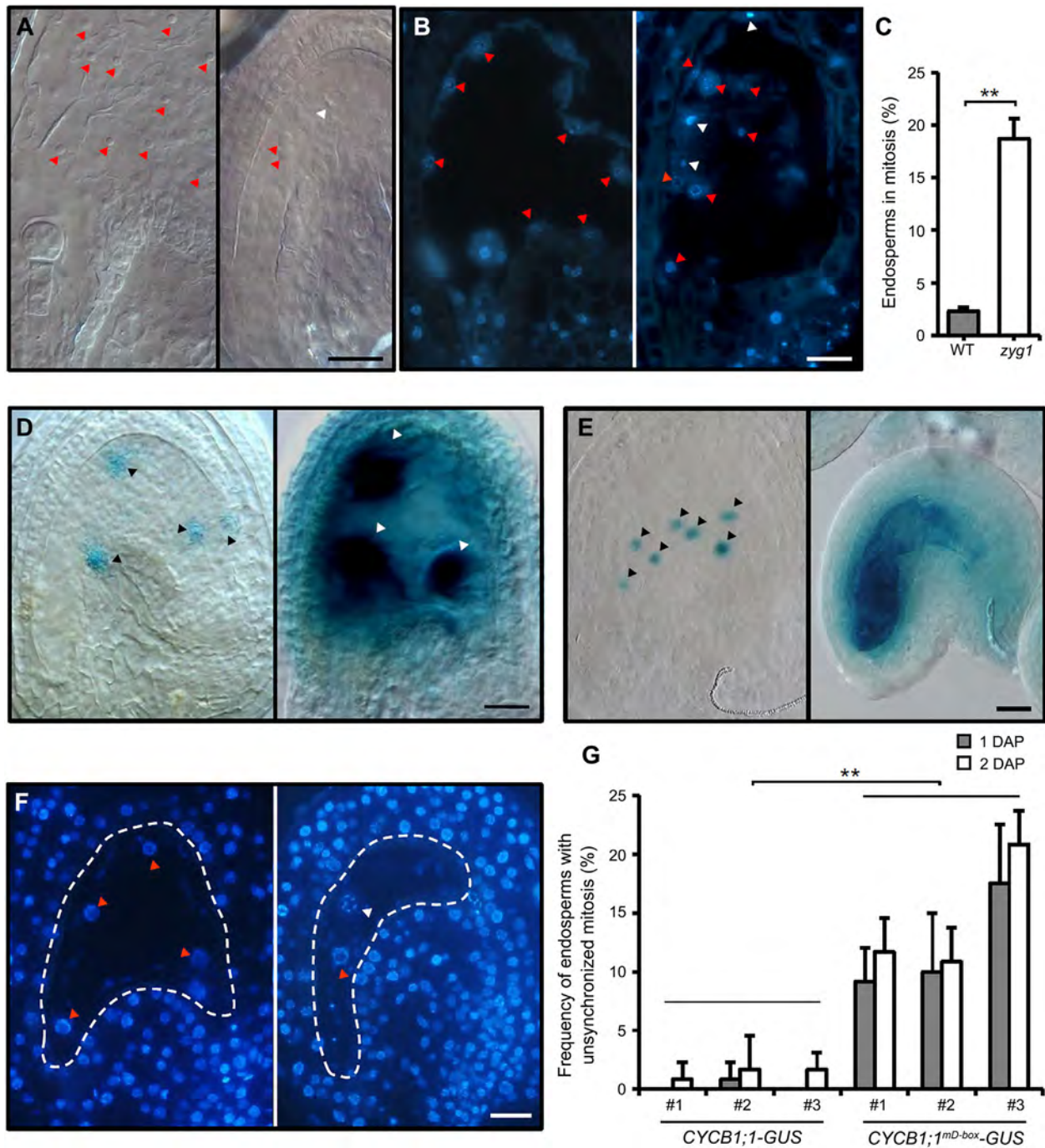


**Figure 1. Unsynchronized mitotic divisions and over-accumulation of *CYCB1-GUS* in syncytial *zyg1* endosperms** (A) DIC microscopic observations show unsynchronized mitosis in a *zyg1* endosperm (right), compared to the wildtype (left). Interphase nuclei are indicated by red arrowheads and mitotic figures are indicated by white arrowheads. Scale bar, 20  $\mu$ m. (B) DAPI staining shows that both interphase (red arrowheads) and mitotic (white arrowheads) nuclei were present in the same *zyg1* endosperm (right), compared to synchronized mitosis in the wildtype endosperm (left). Scale bar, 30  $\mu$ m. (C) Frequencies of endosperms with mitotic figures in the wildtype ( $n = 412$ ) and *zyg1* ( $n = 176$ ). Error bars represent standard deviation, and statistical analysis was performed using a two-tailed Student's *t*-test (\*\* $P < 0.01$ ). (D) GUS staining of endosperms from the wildtype (left) and *zyg1* (right) ovules, both carrying a homozygous *CYCB1-GUS* construct. Note the GUS over-accumulation phenotype (white arrowheads) in arrested *zyg1* endosperms ( $n = 106$ ), compared to the weak and dotted GUS staining (black arrowheads) in the wildtype ( $n = 268$ ). Scale bar, 30  $\mu$ m. (E) Elevated and defused GUS signal in an ovule from

Since APC11 is able to ubiquitinate cyclin B1;1 (CYCB1;1) to promote cyclin B1;1 degradation (Guo et al. 2016), we investigated whether the unsynchronized nuclear division observed in *zyg1* endosperms was also due to impaired cyclin B1;1 degradation. A *pDD7:CYCB1;1<sup>mD-box</sup>-GUS* construct, carrying an endosperm-specific promoter *pDD7*-driven expression of cyclin B1;1 with a mutated D-box fused with a *GUS* reporter gene at its C-terminus (Steffen et al. 2007), was used to transform the wildtype *Arabidopsis* (Col-0). Previous studies showed that the mutation in the D-box compromised the degradation of the CYCB1;1<sup>mD-box</sup>-GUS protein (Guo et al. 2016). Construct of *pDD7:CYCB1;1-GUS* with a native cyclin B1;1 expressed under the same promoter was used as a control.

GUS assay performed in ovules excised at 1 DAP revealed a strong GUS signal in endosperms of T1 plants carrying *pDD7:CYCB1;1<sup>mD-box</sup>-GUS*, compared with faint and dotted GUS expressions in the endosperm of plants carrying *pDD7:CYCB1;1-GUS* (Figures 1E, S2), suggesting that degradation of the CYCB1;1<sup>mD-box</sup>-GUS fusion protein was indeed compromised. Ovules at 2-DAP were excised from transgenic plants carrying *pDD7:CYCB1;1<sup>mD-box</sup>-GUS*, embedded in Technovit, sectioned to 5  $\mu\text{m}$  in thickness, and stained with DAPI. Microscopic examination of these sections revealed a severe defect in cell cycle synchronization. Unlike the synchronized mitosis observed in the wildtype, nuclear divisions in these endosperms varied greatly in mitotic phase (Figure 1F, G), similar to what was observed in *zyg1* endosperms. Such a defect was not observed in plants carrying *pDD7:CYCB1;1-GUS* (Figure 1F, G), suggesting that expressing CYCB1;1<sup>mD-box</sup>-GUS in endosperm disrupted the synchronization of its nuclear divisions.

Given that APC11 is one of the 13 subunits in APC/C that regulates cell cycle progression (Heyman and De Veylder 2012), we investigated whether the

unsynchronized mitotic division in *zyg1* endosperms was due to a general defect in the APC/C. It has been reported that APC1 and APC4 are critical for gametogenesis and early embryogenesis in *Arabidopsis* (Wang et al. 2012, 2013), but no detailed phenotypic analyses have been performed in endosperms. We observed that nuclear divisions in the syncytial endosperms of *apc1-1* and *apc4-3* mutants were indeed not synchronized (Figures 2A–C, S3A–G), suggesting that APC/C is essential for synchronized nuclear divisions in the syncytial endosperm.

To determine whether APC/C also plays a role in cell cycle synchronization in somatic cells, transgenic plants that carry artificial microRNA targeted to APC11, expressed under the control of the *CaMV 35S* promoter (*amiRNA-APC11*), were generated and examined. Among the 204 primary transgenic plants that were obtained, 66 (32.4%) had short-root and stunted leaf phenotypes (Figures 2D–F, S4A). Quantitative RT-PCR analyses showed that, compared to the wildtype, the expression level of APC11 in these aberrant plants was significantly reduced (Figure 2G). Using a DIC microscope, we observed that some cells in these cotyledons were multinucleate (Figures 2H–J, S4B), suggesting a defect in cytokinesis, as reported in tobacco when non-degradable cyclin B1;1 was expressed (Weingartner et al. 2004). Within these multinucleate cells, mitotic divisions were not synchronized: some nuclei were in the interphase, whereas others were in prophase or metaphase (Figure 2I). This unsynchronized mitosis phenotype was also observed in multinucleate guard cells with abnormal shapes (Figures 2K–M, S4C).

In summary, although many *Arabidopsis* mutants such as *titan*, with defective endosperm development, have been identified (Liu and Meinke 1998), none showed evident defects in cell cycle synchronization in endosperms. Previously, we showed that APC11

transgenic plants carrying *pDD7:CYCB1;1<sup>mD-box</sup>-GUS* (right), compared to a weak and dotted GUS signal (black arrowheads) in an ovule from a transgenic wildtype plant carrying *pDD7:CYCB1;1-GUS* (left). Scale bar, 20  $\mu\text{m}$ . (F) DAPI-stained ovule sections from transgenic plants carrying *pDD7:CYCB1;1<sup>mD-box</sup>-GUS* (right) showing mixed mitotic figures in different phases (white and red arrowheads) within the same endosperm, compared to synchronized mitotic figures (red arrowheads) in endosperms of a plant carrying *pDD7:CYCB1;1-GUS* (left). Scale bar, 20  $\mu\text{m}$ . (G) Frequency of ovules with unsynchronized endosperm nuclei in transgenic plants carrying *pDD7:CYCB1;1-GUS* or *pDD7:CYCB1;1<sup>mD-box</sup>-GUS* ( $n = 120$  each). Data were collected from three independent plants for each construct, with ovules at 1 and 2 DAP. Error bars represent standard deviation, and statistical analysis was performed using a two-tailed Student's *t*-test (\*\* $P < 0.01$ ).

interacts directly with cyclin B1 to promote the degradation of cyclin B1, and ultimately initiate zygote division (Guo et al. 2016). In this study, we observed that the mutation in *APC11/ZYG1* led to cyclin B1 over-accumulation and unsynchronized mitosis in endosperms. Such defective cell cycle synchronization was also observed in the endosperm when genes coding other two APC subunits, *APC1* and *APC4*, were mutated, and in somatic cells when *APC11* was downregulated using microRNA targeted to *APC11*. Similarly, transgenic expression of a non-degradable cyclin B1 in endosperms led to cyclin B1 over-accumulation and unsynchronized mitosis in the syncytial endosperm.

In addition to the demonstrated roles of APC/C in cyclin degradation and cell cycle progression in yeast and animals (Cross 2003; Pines 2011), we propose that APC/C may coordinate the cell cycle synchronization of multiple nuclei in a shared cytoplasmic environment through cyclin B1 degradation. It is striking that embryo development in the *zyg1* mutant is arrested immediately after the zygote is formed, whereas endosperm development in the same mutant is able to continue through several cycles of unsynchronized mitosis. This could be due to the presence of residual parental *APC11/ZYG1* protein and/or transcript in the central cell, which would be depleted to a level below a threshold after

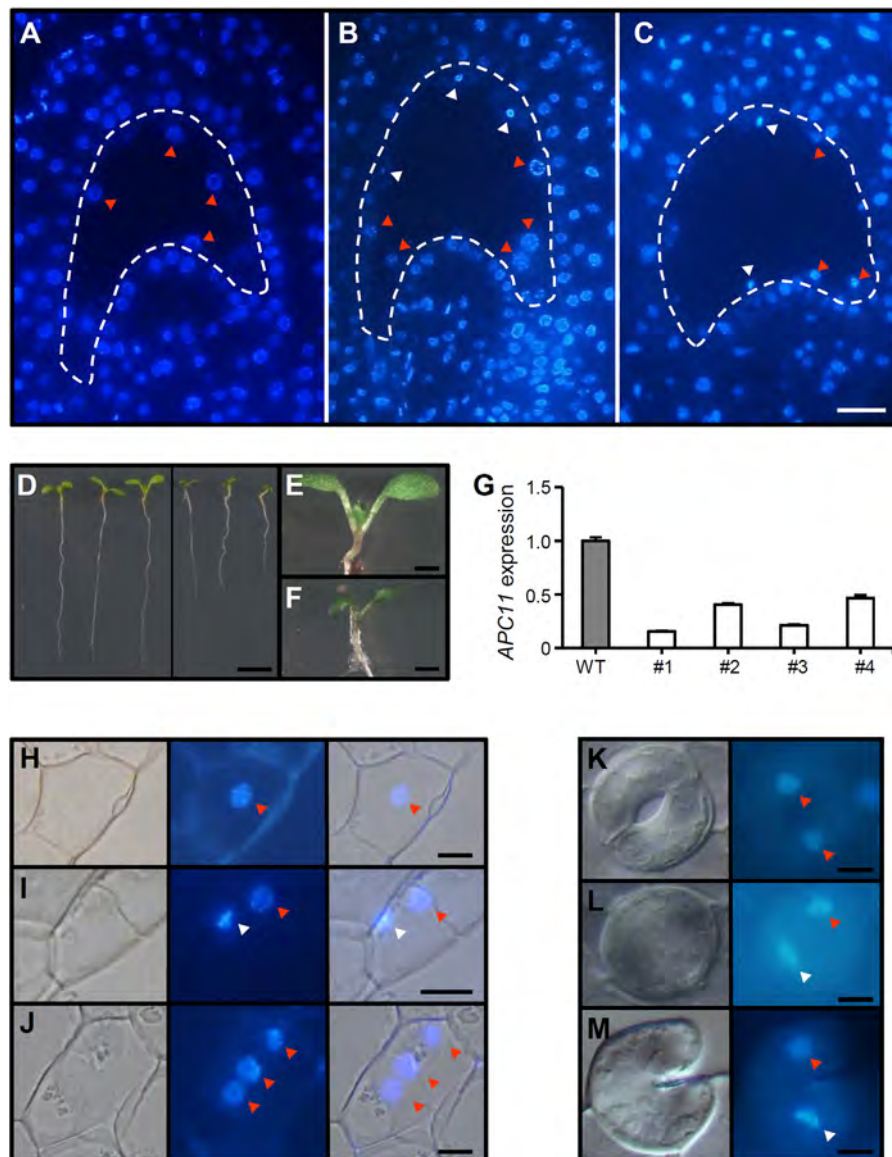


**Figure 2 Continued.**

several rounds of mitosis, at which point unsynchronized nuclear divisions may occur. This hypothesis is supported by the observation that there was an increase in unsynchronized mitosis during the later stage of *zyg1* endosperm development. Whether the same machinery functions in cell cycle synchronization in coenocytic embryos of animals, such as *Drosophila*, remains to be investigated.

## MATERIALS AND METHODS

### Plant materials and growth conditions

*Arabidopsis thaliana*, ecotype Col-o, *ZYG1/zyg1* (Col-o) (Guo et al. 2016), *APC1/apc1-1* (Col-o) (Wang et al. 2013), and *APC4/apc4-3* (Col-o) (Wang et al. 2012) were used in this study. The artificial microRNA construct *CSHL\_041197* (*amiRNA-APC11*) (Schwab et al. 2006) was obtained from the Arabidopsis Biological Resource Center (ABRC) at Ohio State University, and transformed into Col-o to generate *amiRNA-APC11* transgenic plants. All plants were grown at  $20 \pm 2^\circ\text{C}$  in a growth room with 16 h of light ( $100 \mu\text{mol photons m}^{-2}\text{s}^{-1}$ ) per day.

### Plasmid construction and transformation

To generate *CYCB1;1<sup>mD-box</sup>*, *cyclin B1;1* genomic DNA was amplified and introduced into *pEASY-Blunt* (TransGen), and then the sequence coding D-box was altered by PCR mutagenesis, in which two highly conserved amino acids were changed to alanine (from

RQVLGDIGN to AQVAGDIGN), generating *pEASY-Blunt-CYCB1;1<sup>mD-box</sup>*, as described previously (Guo et al. 2016). For endosperm-specific expression, the 1,957 bp *DD7* promoter (Steffen et al. 2007) driven expressions of *CYCB1;1* or *CYCB1;1<sup>mD-box</sup>* were inserted into *pGreenII*, with a *GUS* in-frame fused to their C-termini, to generate *pDD7:CYCB1;1-GUS* or *pDD7:CYCB1;1<sup>mD-box</sup>-GUS*, respectively. Primers used are listed in Table S1. All constructs were transformed into *A. thaliana* (Col-o) via the floral dip method.

### Microscopic and histological analyses

For examination of mitotic divisions in endosperms or cotyledons, samples were embedded in Technovit (Kulzer), sectioned and stained with DAPI. For phenotypic analyses of stomata, 2-week-old cotyledons were treated with 75% ethanol overnight at room temperature until the chlorophyll was removed. The samples were then rehydrated with a series of ethanol concentrations (40%, 20% and 10%) for 15 min each, and then placed in 5% ethanol and 25% glycerol for 30 min. The leaves were mounted in 50% glycerol and stained with DAPI. *GUS* assay was performed as described previously (Xu et al. 2005). A microscope (Eclipse 80i, Nikon) equipped with DIC and fluorescence was used to obtain the micrographs.

### Quantitative RT-PCR analysis

Total RNAs were isolated from seedlings using the Plant Total RNA Purification Kit (GeneMark), and reverse transcribed with the FastQuant RT Kit (TIANGEN)

**Figure 2. Unsynchronized mitosis in *apc1-1* and *apc4-3* endosperms, and in multinucleated somatic cells in *amiRNA-APC11* transgenic plants**  
**(A–C)** DAPI-stained ovule sections from wildtype, *apc1-1* and *apc4-3* plants, showing both interphase (red arrowheads) and mitotic nuclei (white arrowheads) in the same endosperm. Scale bar, 20  $\mu\text{m}$ . **(D–F)** Seedlings carrying *amiRNA-APC11* had short-root and wrinkled cotyledon phenotypes (right), compared to the wildtype (left). Scale bar, 5 mm for **(D)**. Two enlarged inserts showed wrinkled **(F)** and wildtype **(E)** cotyledons. Scale bars, 1 mm for **(E)** and **(F)**. **(G)** The level of *APC11* expression was reduced significantly in the four independent lines (1, 2, 3 and 4) carrying *amiRNA-APC11*, compared to the wildtype. Error bars represent standard deviation. **(H–J)** Multinucleated cells observed under DIC (left), DAPI fluorescence (middle) or merged (right) in the cotyledon of *amiRNA-APC11* transgenic plants **(I and J)**. Note that some nuclei were in interphase (red arrowheads), while others were in mitotic phase (white arrowheads) **(I)**, compared to the single-nucleated cell in the wildtype **(H)**. Scale bars, 10  $\mu\text{m}$ . **(K–M)** Abnormal stomata with round- or heart-shaped guard cells **(L and M)** were observed in epidermis of *amiRNA-APC11* transgenic plants, compared to the wildtype **(G)**. DIC (left) and DAPI fluorescence (right) were used to show a multinucleated stomata cell with mixed cell cycle states: mitotic phase (white arrowheads); interphase (red arrowheads). Scale bars, 10  $\mu\text{m}$ .

according to the manufacturer's instructions. Quantitative RT-PCR was performed with the CFX Connect™ Real-Time PCR Detection System (Bio-Rad) using the SuperReal PreMix Plus Kit (SYBR Green) (TIANGEN). The thermal cycling conditions were 95°C for 15 min; 35 cycles of 95°C for 10 s, 55°C for 20 s, 72°C for 30 s. The relative expression levels were normalized against *EIF4A* using a modified  $2^{-\Delta\Delta C_T}$  method (Livak and Schmittgen 2001). Primers used are listed in Table S1.

### Accession numbers

Sequence data from this article can be found in the EMBL/GenBank under the following accession numbers: *APC11* (At3g05870), *cyclin B1;1* (At4g37490), *APC1* (At5g05560), *APC4* (At4g21530).

## ACKNOWLEDGEMENTS

We thank Lijia Qu for providing *apc1-1* and *apc4-3* seeds, and Huaqin Gong for technical support. This work was supported by “Mechanistic dissection of plant embryo and seed development” project (2014CB943401) from The National Basic Research Program, the Ministry of Science and Technology of China.

**Lei Guo<sup>1</sup>, Li Jiang<sup>††</sup>, Xiu-Li Lu<sup>1</sup> and Chun-Ming Liu<sup>1,2\*</sup>**

1. Key Laboratory of Plant Molecular Physiology, Institute of Botany, Chinese Academy of Sciences, Beijing 100093, China

2. Institute of Crop Sciences, Chinese Academy of Agricultural Sciences, Beijing 100081, China

<sup>†</sup>Present address: Chinese Academy of Fishery Sciences, Beijing 100141, China

\*Correspondence: Chun-Ming Liu (cmliu@ibcas.ac.cn)  
doi: 10.1111/jipb.12641

**Edited by:** Meng-Xiang Sun, Wuhan University, China

**Received** Dec. 17, 2017; **Accepted** Feb. 6, 2018; **Online on** Feb. 9, 2018  
FA: Free Access

## AUTHOR CONTRIBUTIONS

L.G. performed genetic, cytological and histological analyses, L.J. and X.L.L. carried out some histological analyses, C.M.L. designed the experiments and guided the study, L.G. drafted and C.M.L. revised the manuscript.

## REFERENCES

- Colón-Carmona A, You R, Haimovitch-Gal T, Doerner P (1999) Spatio-temporal analysis of mitotic activity with a labile cyclin-GUS fusion protein. **Plant J** 20: 503–508
- Cross FR (2003) Two redundant oscillatory mechanisms in the yeast cell cycle. **Dev Cell** 4: 741–752
- Dumas C, Rogowsky P (2008) Fertilization and early seed formation. **CR Biol** 331: 715–725
- Ferree PL, Deneke VE, Di Talia S (2016) Measuring time during early embryonic development. **Semin Cell Dev Biol** 55: 80–88
- Guo L, Jiang L, Zhang Y, Lu XL, Xie Q, Weijers D, Liu CM (2016) The anaphase-promoting complex initiates zygote division in *Arabidopsis* through degradation of cyclin B1. **Plant J** 86: 161–174
- Hara T, Katoh H, Ogawa D, Kagaya Y, Sato Y, Kitano H, Nagato Y, Ishikawa R, Ono A, Kinoshita T, Takeda S, Hattori T (2015) Rice SNF2 family helicase ENL1 is essential for syncytial endosperm development. **Plant J** 81: 1–12
- Heyman J, De Veylder L (2012) The anaphase-promoting complex/cyclosome in control of plant development. **Mol Plant** 5: 1182–1194
- Liu CM, McElver J, Tzafirir I, Joosen R, Wittich P, Patton D, Van Lammeren AAM, Meinke D (2002) Condensin and cohesin knockouts in *Arabidopsis* exhibit a *titan* seed phenotype. **Plant J** 29: 405–415
- Liu CM, Meinke DW (1998) The *titan* mutants of *Arabidopsis* are disrupted in mitosis and cell cycle control during seed development. **Plant J** 16: 21–31
- Livak KJ, Schmittgen TD (2001) Analysis of relative gene expression data using real-time quantitative PCR and the  $2^{-\Delta\Delta C_T}$  method. **Methods** 25: 402–408
- Pines J (2011) Cubism and the cell cycle: The many faces of the APC/C. **Nat Rev Mol Cell Biol** 12: 427–438
- Schwab R, Ossowski S, Riester M, Warthmann N, Weigel D (2006) Highly specific gene silencing by artificial microRNAs in *Arabidopsis*. **Plant Cell** 18: 1121–1133
- Steffen JG, Kang IH, Macfarlane J, Drews GN (2007) Identification of genes expressed in the *Arabidopsis* female gametophyte. **Plant J** 51: 281–292
- Wang Y, Hou Y, Gu H, Kang D, Chen Z, Liu J, Qu LJ (2012) The *Arabidopsis* APC4 subunit of the anaphase-promoting complex/cyclosome (APC/C) is critical for both female gametogenesis and embryogenesis. **Plant J** 69: 227–240
- Wang Y, Hou Y, Gu H, Kang D, Chen ZL, Liu J, Qu LJ (2013) The *Arabidopsis* anaphase-promoting complex/cyclosome subunit 1 is critical for both female gametogenesis and embryogenesis. **J Integr Plant Biol** 55: 64–74
- Weingartner M, Criqui MC, Mészáros T, Binarova P, Schmit AC, Helfer A, Derevier A, Erhardt M, Bögre L, Genschik P (2004) Expression of a nondegradable cyclin B1 affects plant development and leads to endomitosis by inhibiting the formation of a phragmoplast. **Plant Cell** 16: 643–657
- Xu J, Zhang HY, Xie CH, Xue HW, Dijkhuis P, Liu CM (2005) EMBRYONIC FACTOR 1 encodes an AMP deaminase

and is essential for the zygote to embryo transition in *Arabidopsis*. **Plant J** 42: 743–756

## SUPPORTING INFORMATION

Additional Supporting Information may be found online in the supporting information tab for this article: <http://onlinelibrary.wiley.com/doi/10.1111/jipb.12641/supinfo>

**Figure S1.** Cell cycle synchronization is defective in the *zyg1* endosperm

(A) Number of nuclei in wildtype and *zyg1* endosperms ( $n = 60$  each) at 2.0 and 2.5 DAP. Note the reduced number of endosperm nuclei in *zyg1* compared to the wildtype. (B) Frequencies of mitotic nuclei in endosperms of wildtype and *zyg1* mutant ( $n = 60$  each) at 1.0, 1.5, 2.0, and 2.5 DAP. (C) Frequencies of unsynchronized mitotic divisions in wildtype and *zyg1* endosperms ( $n = 60$  each) at 1.0, 1.5, 2.0, and 2.5 DAP. Error bars represent standard deviation, and statistical analysis was performed using a two-tailed Student's *t*-test ( $*P < 0.05$ ;  $**P < 0.01$ ).

**Figure S2.** Transgenic plants carrying *pDD7:CYCB1;1<sup>mD-box</sup>-GUS* showed GUS over accumulation phenotype

Frequency of endosperms displaying GUS accumulation in plants carrying *pDD7:CYCB1;1-GUS* or *pDD7:CYCB1;1<sup>mD-box</sup>-GUS* ( $n > 100$ ). Data were collected from ovules collected at 1 and 2 DAP. Note that plants carrying *pDD7:CYCB1;1<sup>mD-box</sup>-GUS* showed a GUS over accumulation phenotype. Error bars represent standard deviation, and statistical analysis was performed using a two-tailed Student's *t*-test ( $**P < 0.01$ ).

**Figure S3.** Endosperms in *apc1-1* and *apc4-3* mutants showed unsynchronized mitosis phenotype

Frequencies of mitotic figures in endosperms of the wildtype, *apc1-1* (A) and *apc4-3* (B) ( $n = 60$  each) at 2.0 and 2.5 DAP. (C) Frequencies of endosperms with unsynchronized mitotic divisions in the wildtype and *apc1-1* ( $n = 60$  each) at 2.0 and 2.5 DAP. (D) Frequencies of endosperms with unsynchronized mitotic divisions in the wildtype and *apc4-3* ( $n = 60$  each) at 2.0 and 2.5 DAP. Error bars represent standard deviation, and statistical analysis was performed using a two-tailed Student's *t*-test ( $*P < 0.05$ ;  $**P < 0.01$ ). (E–G) DIC microscopic observations showed unsynchronized mitosis in *apc1-1* (F) and *apc4-3* (G) endosperms, compared to the synchronized mitosis in the wildtype endosperm (E). Interphase nuclei are indicated by red arrowheads, and mitotic figures are indicated by white arrowheads. Scale bars, 20  $\mu\text{m}$ .

**Figure S4.** Transgenic plants carrying *amiRNA-APC11* showed short-root, stunted leaf and multinucleated cells with defective cell cycle synchronization

(A) Lengths of primary roots in the wildtype and *amiRNA-APC11* seedlings ( $n = 30$ ) at 5 d after germination. Error bars represent standard deviation, and statistical analysis was performed using a two-tailed Student's *t*-test ( $**P < 0.01$ ). (B) Frequencies of multinucleated cells in cotyledons from the wildtype and three independent *amiRNA-APC11* lines (a, b and c) ( $n = 150$  each). (C) Frequencies of abnormal stomata in cotyledons from the wildtype and three independent *amiRNA-APC11* lines (a, b and c) ( $n = 240$  each).

**Table S1.** Primers used in this study



Scan using WeChat with your smartphone to view JIPB online



Scan with iPhone or iPad to view JIPB online